Gliotactin and Discs large form a protein complex at the tricellular junction of polarized epithelial cells in *Drosophila*

Joost Schulte, Kristi Charish, Jaimmie Que, Sarah Ravn, Christina MacKinnon and Vanessa J. Auld*

Department of Zoology, University of British Columbia, Vancouver, V6T 1Z3, Canada

*Author for correspondence (e-mail: auld@zoology.ubc.ca)

Accepted 9 August 2006
Journal of Cell Science 119, 4391-4401 Published by The Company of Biologists 2006
doi:10.1242/jcs.03208

Summary

The tricellular junction (TCJ) forms at the convergence of pleated septate junctions (SJs) from three adjacent cells in polarized epithelia and is necessary for maintaining the transepithelial barrier. In *Drosophila*, the transmembrane protein Gliotactin was the first identified marker of the TCJ, but little is known about other molecular constituents. We now show that Gliotactin associates with Discs large at the TCJ in a Ca^{2+}-dependent manner. Discs large is essential for the formation of the TCJ and the localization of Gliotactin. Surprisingly, Gliotactin localization at the TCJ was independent of its PDZ-binding motif and Gliotactin did not bind directly to Discs large. Therefore Gliotactin and Discs large association is through intermediary proteins at the TCJ. Gliotactin can associate with other septate junction proteins but this was detected only when Gliotactin was overexpressed and spread throughout the septate junction domain. Gliotactin overexpression and spread also resulted in a reduction of Discs large staining but not vice versa. These results suggest that Discs large participates in different protein interactions in the SJ and the TCJ. Finally this work supports a model where Gliotactin and Dlg are components of a larger protein complex that links the converging SJs with the TCJ to create the transepithelial barrier.

Key words: Septate junction, Tricellular junction, Epidermis, *Drosophila*, Imaginal discs, Dlg, PDZ

Introduction

The formation of septate junctions (SJ) in polarized epithelia such as salivary glands, intestine and epidermis are necessary to maintain the integrity of epithelial barriers in insects. SJ strands or septa form a multi-stranded region just basal to adherens junctions that effectively blocks paracellular flow. In *Drosophila*, two types of SJs, smooth and pleated, have been observed (Tepass and Hartenstein, 1994). Pleated SJs are found in ectodermally derived tissue such as the hindgut, trachea, glia and imaginal discs, whereas smooth SJs are found in endodermally derived tissue such as the midgut. Septate junctions are found in vertebrate systems at the node of Ranvier and share multiple components with insect pleated SJs (Peles and Salzer, 2000).

EM studies determined that pleated SJs are discontinuous and interrupted at the conjunction of three cells by channels at a region termed the tricellular junction (TCJ) (Fristrom, 1982; Noirot-Timothee et al., 1982; Walker et al., 1985). The TCJ forms where the ribbon-like septate junctions make a hairpin turn and run in an apical-basal direction. The permeability barrier at this junction is created by a series of plugs or diaphragms that span the junction and are presumably held in position by interaction with the descending septa from the SJ (Fristrom, 1982; Noirot-Timothee et al., 1982). Gliotactin was the first protein shown to specifically localize to this region in *Drosophila* (Schulte et al., 2003). Gliotactin is a transmembrane protein localized to the TCJ in a number of embryonic tissues including epidermal cells, salivary gland cells and the peripheral glia. Removal of Gliotactin in embryonic epithelia blocks the maturation and consolidation of pleated septate junctions. Septa are still present in Gliotactin mutants, however SJ components such as Neurexin IV and Coracle are spread more basally than in the wild type and the permeability barrier fails to form (Schulte et al., 2003). The TCJ itself is disrupted in Gliotactin mutants leading to the model whereby Gliotactin functions to link the TCJ to the SJ septa. However, the molecular nature of the protein complex that resides at the TCJ is unknown.

Gliotactin is homologous to the vertebrate Neuroligins (Gilbert et al., 2001; Gilbert and Auld, 2005). All members of this family contain a highly conserved extracellular serine esterase-like domain, which lacks one of three residues necessary for enzymatic function. This extracellular domain is necessary for Neuroligins to form oligomers and bind their ligands, which are specific splice isoforms of the α- and β-Neurexin 1, 2, 3 genes (Boucard et al., 2005; Dean et al., 2003; Ichtchenko et al., 1995; Ichtchenko et al., 1996). Neuroligin/Neurexin interactions are Ca^{2+} dependent and the putative Ca^{2+}-binding region is conserved in the extracellular domain of Neuroligins and Gliotactin (Tsigelny et al., 2000). In addition to these extracellular domains, all members of this family of proteins have a conserved PDZ-binding motif at their immediate C-terminus suggesting this region is important for protein function. The vertebrate Neuroligins found at CNS synapses, have been shown to bind to and colocalize with a number of proteins that contain PDZ domains including CIPP

(Kurschner et al., 1998), S-SCAM/Magi (Iida et al., 2004) and PSD-95 (Irie et al., 1997). Given these highly conserved protein domains, the aim of this investigation was to investigate potential interactions between Gliotactin and the *Drosophila* PSD-95 homologue, Discs large (Dlg), at the TCJ and the role of this complex in larval septate junction formation.

Results

Gliotactin is localized to the TCJ in a wide range of larval tissues

Our initial studies on Gliotactin function and localization were carried out in developing embryonic epithelia (Schulte et al., 2003). However, these cells are small in size making it difficult to determine the precise nature of Gliotactin distribution at the TCJ. To obtain a better understanding of the localization of Gliotactin with respect to junction formation, we analyzed a range of epithelial tissues in the third larval instar (Fig. 1). Gliotactin expression occurs through all larval stages at the TCJ in a wide range of tissues requiring permeability barriers including epidermis, trachea, salivary gland (arrows, Fig. 1A-E), but not in tissues that contain smooth septate junctions (data not shown). The large cells show that the TCJ structure can be extensive and span several micrometers. Gliotactin is also expressed in imaginal discs at the TCJs of both the peripodial and columnar cells (Fig. 1F-H). In these tissues Gliotactin expression was coincident with known SJ proteins such as Coracle, Neuroglian, Dlg and the Na^+/K^+ ATPase α subunit as the septa converge at the TCJ (Fig. 1). The large cells that form the larval epidermis, trachea, salivary glands and peripodial cells of the imaginal discs were ideal for analyzing the distribution of these proteins (Figs 1 and 2). The distinct morphology and extension of the pleated SJ in the basolateral domain can easily be seen (Fig. 2C) as can the distribution of Gliotactin at the TCJ (Fig. 2A,B). However, a low level of Gliotactin can often be seen throughout the SJ domain (Fig. 2A,B), suggesting that Gliotactin may be part of septate junctions but specifically concentrated at the TCJ.

Gliotactin distribution at the TCJ was concentrated in discrete regions, the morphology of which varied depending on the cell type analyzed. For instance, epidermal cells had a punctate staining ranging from one to three puncta per cell corner (arrows, Fig. 2A,B). However, the trachea and peripodial cells of the wing imaginal disc had a ribbon-like domain of Gliotactin expression at the TCJ (arrows, Fig. 1C,D,F). This difference in Gliotactin distribution may be due to differences in cell morphology. For instance the peripodial cells form a squamous epithelia of only a few micrometers thick compared with the depth of the cells of the epidermis, salivary gland and disc columnar cells. Gliotactin positioning in the TCJ suggests that it may form the link between the proteins that form the plug of the TCJ and the descending septate junctions.

Gliotactin overlaps Dlg staining compared with other SJ markers

We took advantage of the large size of the TCJ in larval epidermal and peripodial cells to visualize the location of Gliotactin compared with other SJ proteins. Dlg staining consistently overlapped with Gliotactin at the TCJ compared with another SJ marker, Neuroglian (Fig. 2A,B,D-F: compare Dlg, Gliotactin with Neuroglian). Additionally Dlg in general had a distinct pattern throughout the SJ domain. Although Coracle and Neuroglian were almost identical in the pattern of expression around the septate junction (asterisk, Fig. 2C), Dlg consistently failed to overlap completely with Neuroglian (asterisk, Fig. 2D). This suggests that Dlg may participate in distinct protein complexes in the TCJ and SJ domains compared with other SJ proteins.

Gliotactin is in a protein complex with Dlg

Gliotactin appears to overlap with Dlg at the TCJ and to a lesser extent with other core SJ proteins (Neuroglian, Neurexin IV, Coracle). Therefore we wanted to determine if Gliotactin physically associates with these proteins. Using immunoprecipitation assays on adult membrane proteins, we found that Gliotactin and Dlg are part of the same protein complex (Fig. 3A). Immunoprecipitations using the Gliotactin monoclonal antibody isolated a protein complex containing a

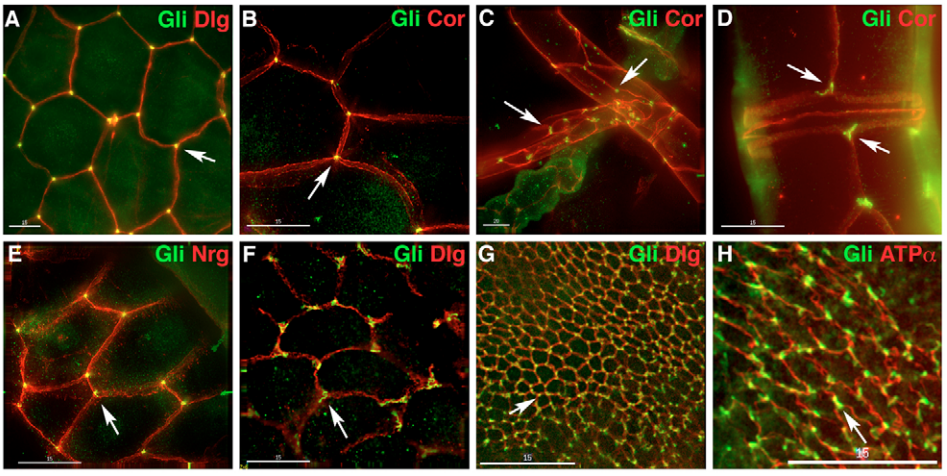

Fig. 1. Gliotactin is found at TCJs in numerous larval tissues. (A,B) Epidermal cells stained with Gliotactin at the TCJ. Gliotactin (green) is concentrated at the TCJ (arrows) compared with Dlg (red) in A or Coracle (red) in B, which label the entire SJ domain. (C,D) Tracheal cells labeled with Gliotactin at the TCJ between tracheal cells. Gliotactin (green) and Coracle (red) co-staining shows the concentration of Gliotactin at the TCJ (arrows). (E) Salivary gland cells labeled with Gliotactin (green) and Neuroglian (red). Gliotactin at the TCJ has a punctate pattern (arrow). (F) Peripodial cells from the wing imaginal disc labeled with Gliotactin (green) and Dlg (red) showing the ribbon like structure of the TCJ (arrows) which extend over several microns. (G,H) Columnar epithelial cells from wing imaginal discs labeled with Gliotactin (green) and Dlg (red) in G and the Na^+/K^+ ATPase α subunit (red) in H. Despite their small size, the TCJ is distinguishable from the rest of the septate junction domain (arrows). Bars, 15 μm (A,B,D-H); 20 μm (C).

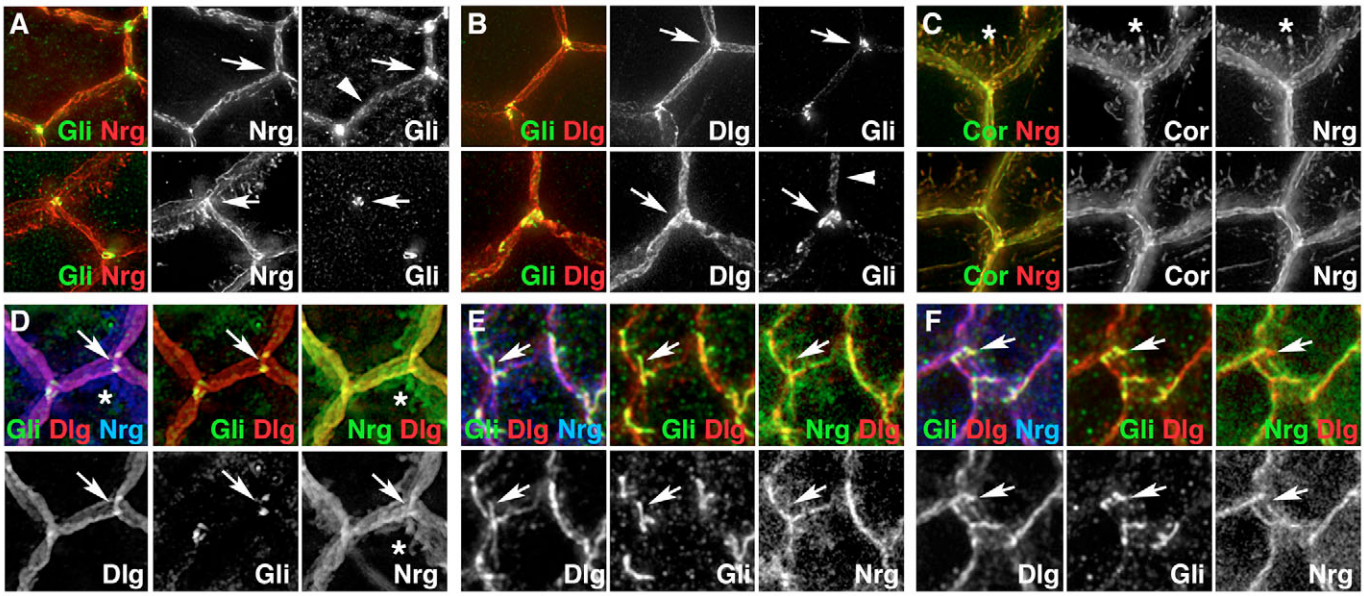

Fig. 2. Gliotactin is distributed with Dlg in a range of TCJs. (A) Gliotactin (green) and Neuroglian (red) have only a small degree of overlap at the TCJ in epidermal cells. The merged image is followed by Neuroglian (red channel) and then Gliotactin (green channel) staining in grayscale. At the TCJ the degree of Neuroglian staining is far less than Gliotactin (arrows). Gliotactin can be seen in the SJ domain though at much lower levels than at the TCJ. (B) Gliotactin (green) and Dlg (red) overlap in the TCJ of epidermal cells. Dlg, like Gliotactin, has a greater degree of labeling at the TCJ (arrows). (C) Coracle (green) and Neuroglian (red) overlap in epidermal cells. The merged image is followed by Coracle (green channel) and Neuroglian (red channel) in grayscale. Both proteins show a distinct morphology with ruffled edges (asterisks) in these cells, perhaps reflecting the pleated nature of these septate junctions. (D) Gliotactin compared with Dlg and Neuroglian at the epidermal cell TCJ. For each set of panels the merged image (Gliotactin, green; Dlg, red; Neuroglian, blue) is followed by: Gliotactin (green) and Dlg (red), Neuroglian (green) and Dlg (red). On the bottom row: Dlg (red channel), Gliotactin (green channel) and Neuroglian (blue channel) are in grayscale to show the individual patterns. Gliotactin and Dlg have a greater degree of staining at the TCJ compared with Neuroglian (arrows). Dlg is distinct in pattern from Neuroglian at the SJ, where Neuroglian has a ruffled morphology (asterisks) compared with Dlg. (E,F) Gliotactin compared with Dlg and Neuroglian at the peripodial cell TCJ. For each set of panels the merged image (Gliotactin, green; Dlg, red; Neuroglian, blue) is followed by: Gliotactin (green) and Dlg (red), Neuroglian (green) and Dlg (red). Dlg (red channel), Gliotactin (green channel) and Neuroglian (blue channel) are in grayscale to show the individual patterns. Gliotactin and Dlg have a greater degree of overlap at the ribbon-like TCJ compared with Neuroglian (compare arrows in panels).

number of Dlg isoforms, including ~120 kDa, ~100 kDa and ~87 kDa isoforms (arrows, Fig. 3A). Interestingly, only those assays carried out in the presence of 0.1 μM or 0.2 μM Ca^{2+} pulled down Dlg in association with Gliotactin. However the same assays also showed that the ability to pull down Gliotactin was also Ca^{2+} dependent (0.05 μM and above) (Fig. 3A). This suggested that access of the monoclonal antibody to the Gliotactin C-terminal epitope maybe Ca^{2+} dependent.

To overcome this problem, we then tested for a direct interaction between Gliotactin and Dlg by using a GST pull-down assay with the entire intracellular domain of Gliotactin fused to GST (GliCter). We tested the ability of this fusion protein to bind to Dlg by testing for interactions in adult membrane preparations. Similar to our immunoprecipitation assays, the GST-GliCter fusion was able to pull down Dlg in a Ca^{2+}-dependent manner (Fig. 3B). This confirmed the Ca^{2+} dependency of the Gliotactin-Dlg immunoprecipitation was not simply an issue with the mAb epitope. In addition the same major isoforms of Dlg were isolated in the GST pull-down assays (arrows, Fig. 3A,B).

To test whether the Gliotactin-Dlg interaction was a direct one, we carried out a GST pull-down assay with an in vitro translation of the Dlg-A isoform (Fig. 3C). We could detect no interaction between Dlg-A and the GST-GliCter fusion. The positive interaction between the Shaker C-terminal domain and Dlg-A (Tejedor et al., 1997) was used as a positive control (Fig. 3C). As PDZ-mediated interactions are not Ca^{2+} dependent (Hung and Sheng, 2002), these results suggest that the association of Gliotactin with Dlg is not through the PDZ-binding motif. To test this we carried out pull-down assays using a GST fusion to the intracellular domain of Gliotactin (GliCter) and to a mutant form lacking the last three amino acids or the PDZ-binding motif (GliΔPDZ) (Fig. 3D). Both forms were able to isolate Dlg from adult membrane preparations again in a Ca^{2+}-dependent manner. This confirms that the association of Gliotactin and Dlg is not dependent on the PDZ-binding motif. Similar Dlg isoforms were isolated with the GST fusion proteins as with the previous pull-down and immunoprecipitation assays (arrows, Fig. 3D). These results suggest that the association of Gliotactin and Dlg in membrane preparations is an indirect one and that the addition of Ca^{2+} triggers Gliotactin binding to an associated protein or protein complex that in turn recruits Dlg.

Surprisingly Dlg was the only SJ protein we assayed that could be isolated in association with Gliotactin. We tested for the presence of Neurexin IV (Fig. 3A) and were unable to detect an interaction even with the addition of Ca^{2+} in adult (Fig. 3A,B) and in embryo (Fig. 5H) membrane preparations.

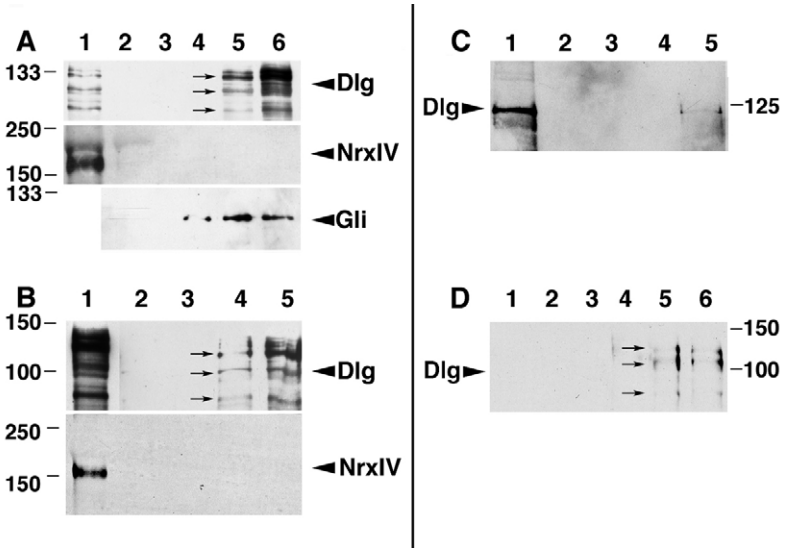

Fig. 3. Endogenous and HA-tagged Gliotactin in protein complexes. (A) Gliotactin is in a Ca^{2+}-dependent protein complex with Dlg but not with Neurexin IV. A Gliotactin mAb was used to immunoprecipitate Gliotactin from membrane preparations isolated from adult flies. The blots were probed with antibodies to Dlg, Neurexin IV and Gliotactin as indicated. The small arrows indicate the major Dlg isoforms isolated (~120 kDa, ~100 kDa and ~87 kDa). 1, membrane preparation; 2, mouse IgG control 0.1 μM Ca^{2+}; 3, Gli mAb no Ca^{2+}; 4, Gli mAb 0.05 μM Ca^{2+}; 5, Gli mAb 0.1 μM Ca^{2+}; 6, Gli mAb 0.2 μM Ca^{2+}. (B) GST pull down using the Gliotactin C-terminal domain recapitulates the immunoprecipitation assays. A GST fusion to the intracellular domain of Gliotactin (GST-GliCter) was used to pull down proteins from adult membrane preparations. The blot was probed with an antibody to Dlg and Neurexin IV. The small arrows indicate the major Dlg isoforms isolated (~120 kDa, ~100 kDa and ~87 kDa). 1, membrane preparation; 2, GST alone 0.1 μM Ca^{2+}; 3, GliCter no Ca^{2+}; 4, GliCter 0.1 μM Ca^{2+}; 5, GliCter 0.2 μM Ca^{2+}. (C) Gliotactin C-terminal domain fails to bind directly to Dlg. A GST fusion to the intracellular domain of Gliotactin (GliCter) and to the intracellular domain lacking the last three amino acids (GliΔPDZ) were used to pull down in vitro translated Dlg. A GST-Shaker C-terminal fusion was used as the positive control. The blot was probed with an antibody to Dlg to detect the in vitro translated product. 1, in vitro translated input; 2, GST alone; 3, GliCter; 4, GliΔPDZ; 5, ShakerCter. (D) GST pull down of Dlg is independent of the PDZ-binding motif. GST-GliCter and GST-GliΔPDZ were used to isolate protein complexes from adult membrane preparations plus or minus Ca^{2+}. The blot was probed with an antibody to Dlg and the interaction with Dlg was Ca^{2+} dependent but independent of the PDZ-binding motif. Similar isoforms were brought down with both forms of Gliotactin (arrows). 1, GST alone no Ca^{2+}; 2, GliCter no Ca^{2+}; 3, GliΔPDZ no Ca^{2+}; 4, GST alone 0.1 μM Ca^{2+}; 5, GliCter 0.1 μM Ca^{2+}; 6, GliΔPDZ 0.1 μM Ca^{2+}.

Similarly, we failed to find Coracle or Neuroglian associated with Gliotactin (data not shown). Therefore the protein associations that underlie Gliotactin function are different from those of other SJ proteins. For instance, in the septate junction, Neurexin IV is a core component that binds to Coracle, Neuroglian and other SJ components (Faivre-Sarrailh et al., 2004; Genova and Fehon, 2003; Llimargas et al., 2004). Conversely Dlg has not been detected to date in these complexes (Hortsch and Margolis, 2003). This also suggests that protein complexes formed at the TCJ may be composed of distinct subsets of SJ proteins.

Loss of Gliotactin in imaginal discs does not disrupt other SJ components

Previous studies on Gliotactin null mutations provided evidence that Gliotactin is not necessary for the formation of the septa per se but rather plays a role in the maturation of the junctional regions during embryogenesis (Schulte et al., 2003). We wanted to test the function of Gliotactin in larval tissues to determine the effects caused by loss of Gliotactin long after the development of septate junctions. Somatic clones of cells lacking Gliotactin were generated using FRT-mediated recombination with a null allele of *Gliotactin* (*Gli*^{dv3}) (Venema et al., 2004) and the subsequent clones were assayed in wing imaginal discs from third instar larvae. In contrast to our previous studies in the embryonic epidermis, loss of function of Gliotactin in imaginal discs had no effect on the localization of SJ components (Fig. 4). Neurexin IV, Neuroglian and Dlg were all normally localized in cells that lacked Gliotactin in the columnar and peripodial cells of the wing imaginal disc. In addition, the apical versus basal localization of these proteins was not altered in mutant versus wild-type cells (Fig. 4B,C). This is in contrast to loss-of-function mutations in many other SJ genes, where removal of one causes the loss of the entire complex. For instance *coracle* null clones result in the absence of Neurexin IV at the membrane and the mislocalization of Neuroglian and Nervana 2 (Genova and Fehon, 2003). Loss of Gliotactin did not affect the localization of the adherens junction marker E-cadherin (Fig. 4I).

Beyond the localization in the septate junction, we assayed cells in *Gliotactin* null clones for the localization of Dlg at the TCJ. Dlg appeared to be concentrated in a pattern similar to wild-type cells in *Gliotactin* null clones (compare arrows in Fig. 4D). This was clear in clones found in peripodial cells where the Dlg pattern at the TCJ is readily assayed (Fig. 4G, compare arrows). In the mutant clones, we were not able to detect Gliotactin expression (Fig. 4F) suggesting that the lack of a SJ phenotype was not due to the retention of Gliotactin protein after clone formation. These results suggest that Gliotactin is necessary for septate junction development and septa compaction but once the SJ domain is established it is stable and does not require Gliotactin to maintain its integrity.

Full-length and Gliotactin ΔPDZ are targeted to the TCJ and rescue the Gliotactin null mutation

To test the functional role of the PDZ-binding motif in Gliotactin, we generated a mutant version of Gliotactin that lacked the PDZ-binding motif along with full-length controls, all under the control of the GAL4 upstream activation sequence (UAS). The mutant GliotactinΔPDZ and a full-length Gliotactin construct were tagged with the HA epitope, which was inserted just before the PDZ motif in the full-length protein (GliΔPDZHA, GliHA, Fig. 5B). In addition, an untagged version of full-length Gliotactin (Gliwt,

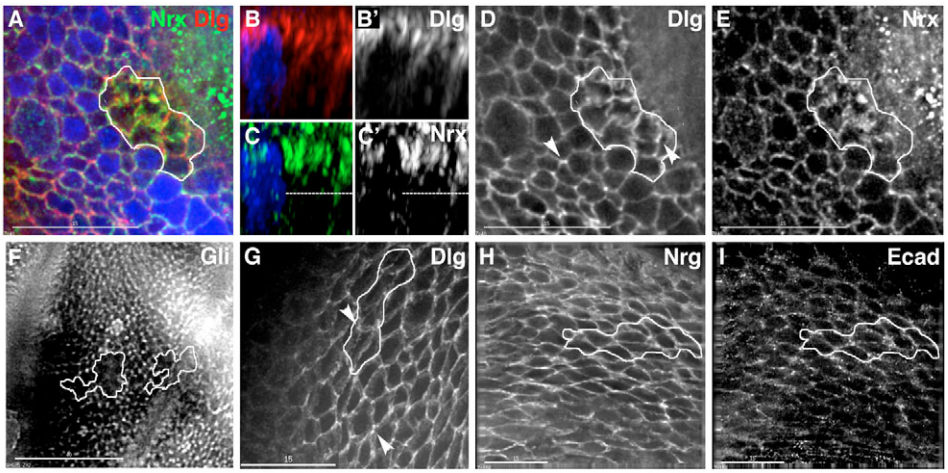

Fig. 4. Gliotactin somatic clones in the wing disc have a normal distribution of septate junction proteins. (A-F) Somatic clones of Gliotactin null mutant in columnar epithelial cells of the wing disc. (A) Clone labeled with Neurexin IV (green) and Dlg (red); mutant cells lack GFP (blue) to show the location of the clone (outlined). (B,C) Side views to show the normal protein distribution in wild-type versus mutant cells. Dlg (B, red) and GFP (B, blue) or Dlg alone (B'). Neurexin IV (C, green) and GFP (C, blue) or Neurexin IV alone (C'). The dashed lines indicate the position of Gliotactin null cells. (D) Dlg (red channel from A) shown in grayscale. Arrowheads indicate the location of the TCJ. (E) Neurexin IV (green channel from A) shown in grayscale. (F) Somatic clones of Gliotactin showing the absence of Gliotactin staining in null clones. (G-I) Somatic clones of Gliotactin mutant cells in peripodial cells of the wing imaginal disc. (G) A clone labeled with Dlg shows normal distribution of Dlg at the TCJ. Compare arrowheads indicating the TCJ in the clone with wild-type cells. (H) Clone of Gliotactin mutant cells labeled with Neuroglian. (I) Clone labeled with E-cadherin. Bars, 15 μm (A-E, G-I); 40 μm (F).

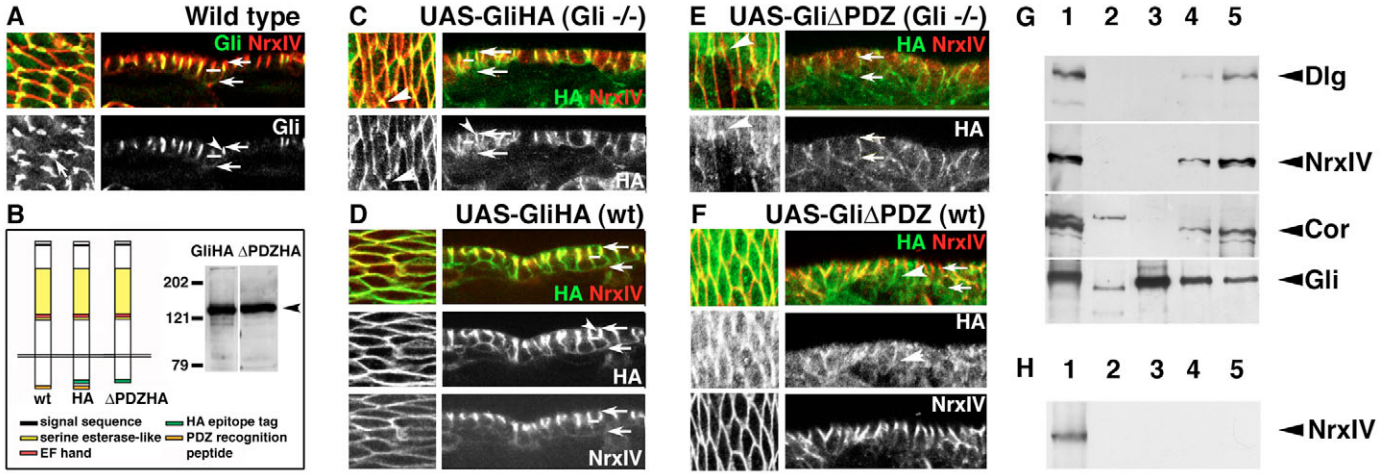

Fig. 5. Wild-type and ΔPDZ Gliotactin are localized correctly to the TCJ. Embryonic epithelia were stained with anti-Gliotactin (green) or anti-HA (green) to show the distribution of wild-type protein or the different transgene proteins. Neurexin IV (red) was used to label the SJ domain. Each panel has en face and longitudinal views to show the distribution of Gliotactin to the TCJ. Arrows indicate the extent of the apical versus basal boundaries of the epidermis. (A) Wild-type embryonic epidermis showing the normal distribution of Gliotactin (green) and Neurexin IV (red). (B) Diagrams of the different Gliotactin constructs used including the untagged full-length (wt), HA-tagged full-length (HA or GliHA) and HA-tagged mutant lacking the last three amino acids (ΔPDZHA). The different domains of the Gliotactin protein and location of the HA tag are indicated. The HA-tagged constructs generated proteins of the expected size when expression was driven in embryos with daughterless-GAL4. (C-F) Expression of transgenic Gliotactin in embryonic epidermis using the daughterless-GAL4 driver line. An antibody to HA was used to detect the expression of the tagged Gliotactin proteins (green) and Neurexin IV (red) was used to mark the SJ domain. (C) Expression of full length Gliotactin (GliHA) in a Gliotactin null background. The full-length protein is highly concentrated at the TCJ. (D) Expression of a full-length Gliotactin (GliHA) in a wild-type background. When overexpressed Gliotactin spreads around the periphery of the cell throughout the SJ domain. The majority of the Gliotactin protein remains in the plane of the SJ domain (arrowhead) with a small amount of basolateral spread (between the two arrows). (E) Expression of GliotactinΔPDZ (GliΔPDZ) in a Gliotactin null background. The GliotactinΔPDZ protein is also highly concentrated at the TCJ. The arrows indicate the extent to which Gliotactin expression spreads in a basolateral direction. (F) Expression of GliotactinΔPDZ (GliΔPDZ) in a wild-type background. The GliotactinΔPDZ protein spreads throughout the SJ domain. The arrows indicate the extent that Gliotactin expression spreads in a basolateral direction. (G) Overexpressed Gliotactin forms a Ca^{2+}-dependent complex with Dlg and other SJ proteins. An anti-HA antibody was used to isolate the tagged full-length Gliotactin from embryos. Membrane preparations were isolated from 12- to 24-hour embryos containing the daughterless-GAL4 driving the UAS-Gliotactin HA-tagged transgene. The blots were probed with antibodies to Dlg, Neurexin, Coracle and Gliotactin. 1, membrane preparation; 2, IgG serum control; 3, HA mAb no Ca^{2+}; 4, HA mAb 0.1 μM Ca^{2+}; 5, HA mAb 0.5 μM Ca^{2+}. (H) Gliotactin mAb was used to immunoprecipitate Gliotactin from wild-type embryos and the blot was probed with an antibody to Neurexin IV. Note the lack of Neurexin IV association with Gliotactin in the wild type versus Gliotactin overexpressing embryos. 1, membrane preparation; 2, IgG control; 3, Gli mAb no Ca^{2+}; 4, Gli mAb 0.1 μM Ca^{2+}; 5, Gli mAb 0.2 μM Ca^{2+}.

Table 1. Rescue of *Gli$^{\Delta 45}$* embryonic lethality with the Gal4/UAS expression system using various UAS-Gli constructs

GAL4 driver	UAS-Gli construct	Genotype of rescued embryos	Rescue of embryonic lethality	% Escapers	Cellular distribution	% With leg defects
No driver	wt#2	*w; Gli$^{\Delta 45}$,UAS-Gli$^{wt\#2}$/ Gli$^{\Delta 45}$*	No	–	–	–
daGAL4	wt#2	*w; Gli$^{\Delta 45}$,UAS-Gli$^{wt\#2}$/ Gli$^{\Delta 45}$; daGAL4/+*	Yes	100	TCJ	58 (*n*=50)
daGAL4	wtHA#3	*w; Gli$^{\Delta 45}$,UAS-Gli$^{wtHA\#3}$/ Gli$^{\Delta 45;}$ daGAL4/+*	Yes	100	TCJ	50 (*n*=50)
daGAL4	PDZΔHA#1	*w; Gli$^{\Delta 45}$/ Gli$^{\Delta 45}$; daGAL4/UAS-gli $^{PDZ\Delta HA\#1}$*	Yes	84	TCJ	100 (*n*=42)

TCJ, tricellular junction.

Fig. 5B) was generated to ensure the tag did not interfere with function. To test for Gliotactin function in embryonic tissues, expression was driven using daughterless-GAL4 which has expression in multiple tissues including epidermis, salivary glands, and glia (Cronmiller and Cummings, 1993). Western analysis confirmed that proteins of the expected molecular weight were produced (Fig. 5B). Each line was crossed into a *Gliotactin* null background, containing the daughterless GAL4 line and the rescue ability of each construct was tested (Table 1). Embryos that lack Gliotactin expression are paralyzed and die at the final stages of embryogenesis (Auld et al., 1995). Both full-length constructs were able to fully rescue the lethality of the *Gliotactin* mutant, even to the extent that viable fertile adults were generated (Table 1). Surprisingly the ΔPDZ form of Gliotactin was also capable of rescuing to adult stages. This was unexpected given the degree of conservation of the PDZ-binding motif in all members of this family of proteins. However, in this case, the adult flies generated had more severe phenotypes, such as a greater penetrance of leg defects and failure to inflate their wings. The leg defects observed in the rescued adults were similar to those seen in homozygotes of hypomorphic *Gliotactin* alleles (D. R. Venema and V.J.A., unpublished results). These defects include shortened tibia, ectopic and fused joints. This suggested that either the levels of the ΔPDZ protein were not sufficient to rescue to the same degree as the wild-type construct or that the loss of the PDZ-binding motif does affect an aspect of Gliotactin function.

We then tested to see if the mutant and wild type forms of Gliotactin would be correctly targeted to the TCJ (Fig. 5). When expressed in a *Gliotactin* null background using the daughterless-GAL4 driver, both full-length and ΔPDZ Gliotactin became localized to the TCJ in embryonic epithelia (arrowheads, Fig. 5C,E). This suggests that the PDZ-binding motif is not necessary for localization to the TCJ. However although the full-length Gliotactin was correctly localized in the basolateral domain with a strong concentration at the SJ junction, the ΔPDZ construct was not. Rather this protein, although weakly expressed, appeared to be distributed more basolateral in the membrane (arrowhead; compare spread between arrows in Fig. 5E with 5A,C). This suggests that the ΔPDZ protein itself or the septate junctions have spread in the basolateral direction.

Overexpressed Gliotactin spreads throughout the SJ domain

We then tested the effects of driving high levels of mutant or full-length protein in a wild-type background by carrying out the expression experiments at higher temperatures (29°C) to increase the efficiency of GAL4 function. We assayed the distribution of Gliotactin in both embryonic epidermis (Fig. 5D,F) and third instar wing imaginal disc (Fig. 6). Under these conditions, full-length and ΔPDZ Gliotactin were mislocalized around the edges of the cell (Fig. 5D,F; Fig. 6E,F). Gliotactin was concentrated within the SJ domain but could also be found throughout the cell membrane (arrowheads, Fig. 5D,F). The overexpression of Gliotactin in the embryonic epidermis had no effect on the normal localization of Neurexin IV (Fig. 5D,F) or Dlg (Fig. 6E,F).

The localization of Gliotactin in the SJ domain after overexpression suggested that Gliotactin is capable of interacting with pleated SJ components. When Gliotactin expression is analyzed in wild-type larval tissues, overexposure of the staining does indicate a small but detectable level of Gliotactin protein in some pleated septate junctions (arrowheads, Fig. 2A,B). However the immunoprecipitation assays from adult membranes suggest that this interaction is either limited, or at such low levels that it cannot be detected in our assays. To test this possibility, immunoprecipitation assays were carried out on embryonic membranes using an antibody to the HA epitope to isolate overexpressed Gliotactin protein driven using the daughterless GAL4 driver. When overexpressed, Gliotactin does form a detectable protein complex with Neurexin IV and still retains its association with Dlg (Fig. 5G). The formation of this complex is also dependent on the presence of Ca^{2+}. In wild-type embryos, Gliotactin fails to immunoprecipitate Neurexin IV (Fig. 5H) even in the presence of Ca^{2+}. This suggests that Gliotactin can associate with SJ components only when overexpressed and spread throughout the SJ domain. Alternatively the results could mean that Gliotactin normally does interact with SJ domain proteins but at levels that were not detected in wild-type adults or embryos.

Overexpressed Gliotactin downregulates Dlg in imaginal discs

We then tested for potential changes in SJ proteins resulting from the overexpression of Gliotactin. For a better side-by-side comparison to assay changes in protein levels, patched-GAL4 or apterous-GAL4 was used to overexpress Gliotactin in a subset of wing imaginal disc cells. In this way the levels of SJ components can be compared between wild-type and adjacent overexpressed tissue (Fig. 6). Using these strong drivers Gliotactin expression was now throughout the cell membrane with a greater concentration in the apical-SJ domain (Fig. 6B'). Using this approach, it was clear that the levels of Dlg staining were reduced in the presence of excess Gliotactin (Fig. 6A-B). The reduction of detectable Dlg was most apparent in the basolateral domain below the septate junctions because Dlg levels were downregulated throughout the cell membrane (Fig. 6B'). However Dlg levels were consistently reduced in the SJ domain (arrow, Fig. 6B'). Of interest was that this effect appeared to be specific to Dlg, as Coracle protein levels were

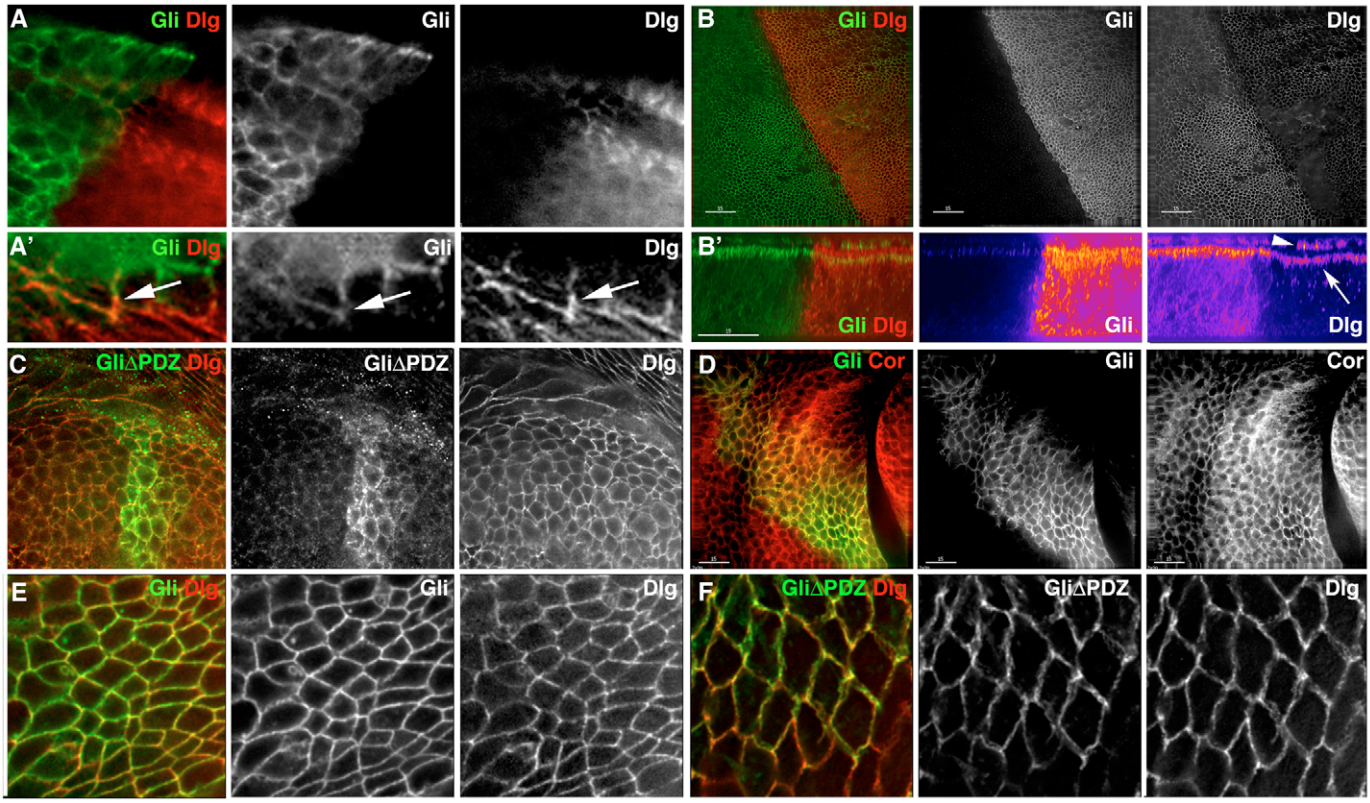

Fig. 6. Ectopic expression of Gliotactin in wing imaginal discs. (A,A') Patched-GAL4 driving full-length Gliotactin. (A) When Gliotactin (green) is overexpressed it is found throughout the cell membrane. There is a reduction in Dlg (red) staining intensity compared with neighbouring wild-type cells. (A') At higher magnification, the Gliotactin overexpressing cells adjacent to wild-type cells clearly show the reduced levels of Dlg compared with non-expressing cells (arrows). The Gliotactin channel (green) was collected at saturating levels of Gliotactin so that the boundary cells could be better assayed. A' has been digitally scaled to 200% of A. (B,B') Apterous-GAL4 driven overexpression of full length Gliotactin. (B) Overexpression of Gliotactin (green) with apterous-GAL4 also results in a reduction of Dlg staining (red). (B') A longitundinal *x*-axis projection of Gliotactin (red) and Dlg (green) and panels showing each individual channel in the LUT scale to indicate intensity of staining. Overexpressed Gliotactin is throughout the cell membrane with the greatest concentration around the apical/SJ region. Dlg expression in these regions is reduced throughout the cell and at the SJ (arrow). The Dlg levels in the overlying peripodial cell layer are not affected (arrowhead) because this cell layer does not express apterous-GAL4. The fire LUT scale ranges from purple (lowest) to white (highest) intensity. (C) Overexpression of GliotactinΔPDZ (green) has no effect on Dlg (red) levels. GliotactinΔPDZ spreads around the cell but fails to downregulate Dlg. (D) Overexpression of full-length Gliotactin (green) had no effect on Coracle (red) levels. (E-F) Overexpression of Gliotactin in embryonic epidermis using 69B-GAL4. (E) Overexpression of full-length Gliotactin (green) had little effect on Dlg (red) levels. (F) Similarly, overexpression of GliotactinΔPDZ (green) had little effect on Dlg (red). Bars, 15 μm.

not affected (Fig. 6D) nor were levels of Neurexin IV (data not shown). These results suggested that the effect of Gliotactin on Dlg may be a direct one, and so to test this, we overexpressed the ΔPDZ Gliotactin construct in wing imaginal discs using the patched-GAL4 line. In these discs Dlg staining was not reduced in intensity (Fig. 6C) in the presence of ΔPDZ Gliotactin. This suggests that the effect of wild-type Gliotactin on Dlg depends on a PDZ-mediated interaction or alternatively that the levels of ectopic GliotactinΔPDZ protein were not sufficient to affect Dlg. This effect on Dlg also appeared to be specific to Gliotactin, because ectopically expressed UAS-NrxIV or UAS-Nrg^{167} using patched-Gal4 had no effect on Dlg levels (data not shown).

Loss of Dlg in imaginal discs blocks Gliotactin localization

Given the association of Dlg and Gliotactin in the TCJ, we wanted to determine the role of Dlg in TCJ formation and Gliotactin localization. Imaginal discs were isolated from homozygous Dlg^{m52} second and third instar larvae and assessed for Gliotactin localization. As a control, imaginal discs were counterstained for Dlg and E-cadherin. Similar to previous observations (Mendoza et al., 2003), we noted some instances of residual Dlg protein in the homozygous mutants (Fig. 7A). In discs with residual Dlg staining (Fig. 7A), Gliotactin is still present but localized away from the TCJ, and E-cadherin is still present in what appears to be puncta at the membrane (arrows). In discs with no residual Dlg staining, Gliotactin is no longer clearly present at the membrane and E-cadherin is mislocalized but often forms puncta (Fig. 7B). This would be expected from the previous TEM analysis of Dlg^{m52} mutants, which show the loss of septate junctions and the formation of ectopic adherens junctions along the basolateral membrane (Woods et al., 1996). This suggests that Dlg is necessary for the correct localization of Gliotactin and its potential associated proteins at the TCJ or conversely for the formation of the TCJ itself.

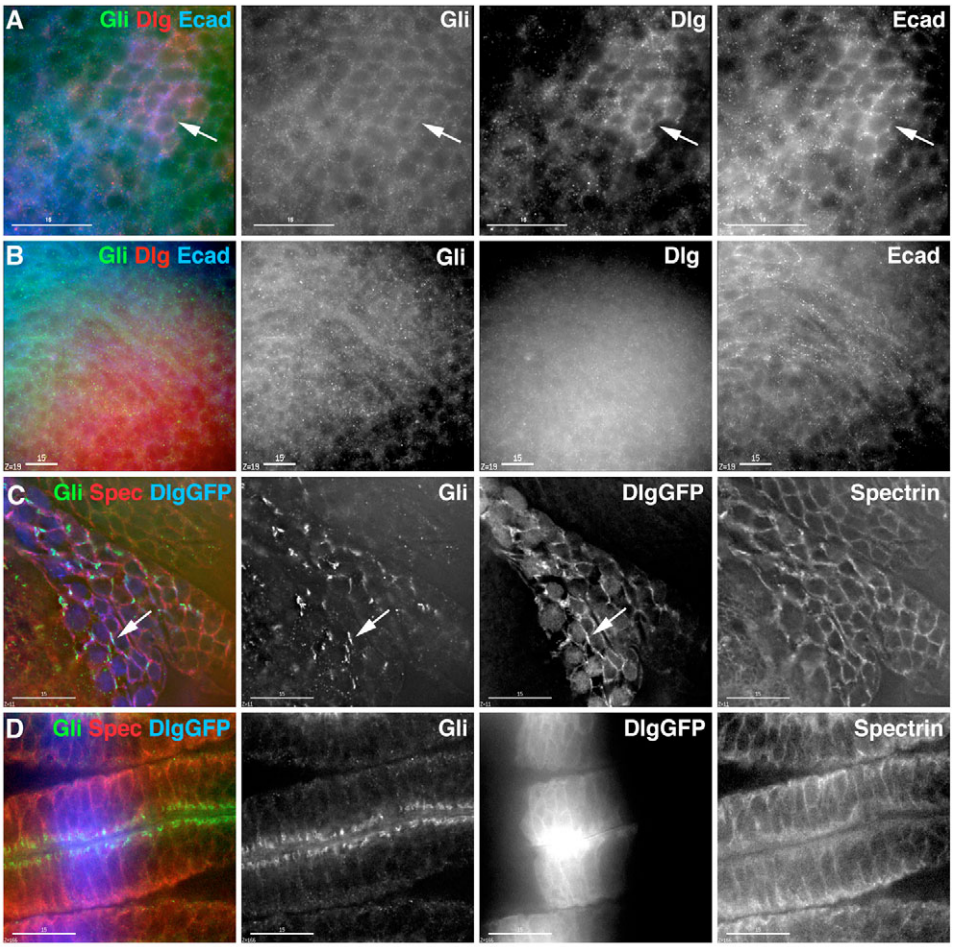

Fig. 7. Loss but not overexpression of Dlg affects Gliotactin localization. (A,B) Gliotactin is mislocalized in Dlg^{m52} mutant imaginal discs. Imaginal discs were isolated from second instar (A) and third instar (B) larvae homozygous from Dlg^{m52} and stained for Gliotactin (green), Dlg (red) and E-cadherin (blue). Arrows in A indicate puncta of staining remaining. (C,D) Gliotactin localization is normal when Dlg is overexpressed. Dlg-A fused to GFP was driven to high levels in the imaginal disc using patched-GAL4. Gliotactin (green) and Spectrin (red) were used to highlight the TCJ and cell boundaries, respectively. DlgGFP (blue) was localized to the TCJ in peripodial cells (C, arrows) and to the SJ domain in columnar epithelia (D). DlgGFP did spread down the SJ domain when overexpressed (D) but had no effect on cell morphology or Gliotactin localization. Bars, 15 μm.

To further elucidate the potential interactions between Gliotactin and Dlg, we overexpressed Dlg with a view to driving up levels throughout the SJ domain and then assessed the effect on Gliotactin protein distribution. Patched-GAL4 was used to drive GFP-tagged Dlg-A (Koh et al., 1999) in a subset of wing imaginal disc cells (Fig. 7C,D). The overexpressed Dlg was targeted to the SJ domain and the TCJ in the peripodial cells (Fig. 7C, arrows) and columnar cells (Fig. 7D) as expected, though Dlg-GFP also spread down the lateral edge of the membrane. Overexpression did not affect cell polarity because E-cadherin was expressed at the appropriate site (data not shown). In these cells Gliotactin localization and levels of expression were not affected suggesting that ectopic Dlg was not sufficient to redirect Gliotactin localization away from the TCJ.

Discussion

Septate junctions and associated TCJs are necessary to form permeability barriers in a wide range of cell types. While recent work has provided much information about the molecular constituents of the septate junction (Hortsch and Margolis, 2003), little is known about the proteins that reside at the tricellular junction (TCJ). Gliotactin was the first protein found to localize in this region, but previous TEM and freeze fracture analysis suggests a large protein complex in this region. Thus Gliotactin is likely to be one of many proteins at the TCJ. Our results suggest that the protein complex is different from those that form the pleated septate junction. Gliotactin does not interact with Neurexin IV or Coracle at levels detectable in our assays. Only when Gliotactin was overexpressed and spread throughout the SJ domain, was an interaction detected. Although we did not test all SJ components, given the core nature of Neurexin IV interactions with other SJ proteins (Faivre-Sarrailh et al., 2004; Genova and Fehon, 2003), it is unlikely that these proteins also interact with Gliotactin to any great extent.

However, Gliotactin did associate with a known SJ component, Discs large. Dlg is clearly localized to the SJ in a distinct domain from Neuroglian and Coracle (Fig. 2C). Dlg is not mislocalized from the SJ in other SJ mutations such as *coracle*, *Neurexin IV* or *Neuroglian* suggesting that it belongs to a separate protein complex in the SJ (Genova and Fehon, 2003), but the protein(s) linking it to the SJ have yet to be identified. On the other hand, Dlg is also localized to the TCJ where it appears to be concentrated in regions that correspond to Gliotactin staining. In addition, Dlg can also be found in the same protein complex as Gliotactin. Dlg is known to have a number of different splice isoforms that can undergo post-translational modification (Woods et al., 1996; Koh et al., 1999; Mendoza et al., 2003). The majority of these would have been detected as we used the monoclonal antibody to the Dlg PDZ2 domain (Parnas et al., 2001). Therefore the identity of those

isoforms that associate with Gliotactin is hard to determine. However bands corresponding to the Dlg-A isoform found in imaginal discs (~120 kDa) (Hough et al., 1997; Thomas et al., 2000) were detected (Fig. 3A). In addition, the Dlg-A GFP fusion associated with the TCJ when expressed in peripodial cells, suggesting that one of the isoforms at the TCJ is Dlg-A. It is possible that the different isoforms seen in our assays represent Gliotactin-Dlg interactions in other tissues such as glial cells, which could easily encompass the 120-130 kDa isoform (Fig. 3A) identified from larval brains (Woods et al., 1996; Mendoza et al., 2003).

Given the high degree of conservation of the PDZ-binding motif in all members of the Gliotactin/Neuroligin family of proteins, it was not surprising to find Dlg in a protein complex with Gliotactin. However, unlike Neuroligin interactions with PSD-95, Gliotactin failed to bind directly to Dlg. What was also unexpected was the fact that the ΔPDZ form of Gliotactin was able to rescue embryonic lethality to adult stages. In addition, Gliotactin was correctly localized to the TCJ with or without this domain. This suggests that another intracellular domain or an extracellular binding interaction may be necessary for Gliotactin localization. This is similar to that observed for the recruitment of Neuroligins in cultured hippocampal neurons where proteins that lack the PDZ-binding motif are correctly localized to the synapse (Dresbach et al., 2004). This suggests that protein interactions other than PSD-95 mediate the synaptic recruitment of Neuroligins. Conversely, other studies have shown that PSD-95 recruits Neuroligin to sites of synaptic development (Prange et al., 2004), though it was not determined if it was a direct or indirect interaction.

From our results, somatic clones in the wing disc lacking Gliotactin appeared to have a normal distribution of Dlg at the septate junction and the TCJ. This suggests that Dlg recruitment to the TCJ is not dependent on Gliotactin. Rather Dlg might bind to an intermediary protein and become recruited to the same complex in the TCJ as Gliotactin. The Gliotactin-Dlg protein complex is independent of the PDZ-binding motif and dependent on Ca^{2+}, further suggesting that Gliotactin requires Ca^{2+} to bind to other TCJ proteins and thus indirectly associates with Dlg. Vertebrate Neuroligins require Ca^{2+} to bind their ligands, the Neurexin 1-3 family of transmembrane proteins (Ichtchenko et al., 1995; Ichtchenko et al., 1996). A potential Ca^{2+}-binding region is conserved in the extracellular domain of Gliotactin (Tsigelny et al., 2000), which leads to the possibility that Gliotactin binds to its ligand in a Ca^{2+}-dependent manner and it is the ligand or associated proteins that recruits Dlg into the complex. However, the GST pull-down assays of the C-terminal domain of Gliotactin also suggest that intracellular protein associations could be Ca^{2+} dependent.

Given the indirect nature of the Gliotactin/Dlg interaction, it was surprising to observe that overexpression of Gliotactin throughout the SJ domain in wing imaginal discs, resulted in the loss of Dlg staining. When overexpressed, full-length Gliotactin associated with other SJ components and Dlg in a Ca^{2+}-dependent manner. This suggests that it is the co-recruitment of other factors that allows Gliotactin to make these new associations and perhaps these cofactors out compete the normal binding site for Dlg or mask the PDZ2 domain, which is the site of antibody binding.

We have combined the observations from this study with previous EM studies to formulate a working model of TCJ protein interactions. The pleated septate junctions make a 90° turn at the boundary of the TCJ (Fristrom, 1982; Noirot-Timothee et al., 1982). As the septa move in an apical-basal direction, they make contact with the plugs or diaphragms that fill the TCJ. Gliotactin is clearly localized to this region, suggesting that Gliotactin forms a complex at the corners of the TCJ. When Gliotactin is overexpressed it shows affinity for the SJ complex and thus could create a link between the proteins of the TCJ plug and the SJ protein complex. Dlg is clearly part of this complex but does not interact directly with Gliotactin and therefore is recruited by other proteins. This points to a larger protein complex that resides at the TCJ whose components beyond Gliotactin and Dlg are still to be discovered.

Materials and Methods

Fly strains

Oregon R and w^{1118} strains are wild-type stocks. $Gli^{\Delta 45}$ and $Gli^{dv3}$are null alleles (Venema et al., 2004). The daughterless-GAL4, patched-GAL4, apterous-GAL4 and 69B-GAL4 are GAL4 insertions lines from the Bloomington stock center. dlg^{m52} (Woods et al., 1996) is a genetic null allele of *dlg*. UAS-DlgGFP is the Dlg-A isoform tagged with GFP (Koh et al., 1999). UAS-Gliwt#2 is untagged full-length Gliotactin, UAS-GliHA#3 is HA tagged full-length Gliotactin, UAS-GliΔPDZHA#1 is HA-tagged Gliotactin lacking the PDZ-binding motif; all were generated as outlined below. The UAS-Neurexin IV line is an EP insertion into Neurexin IV (Nrx^{EP604}). The UAS-Nrg^{167} line is the short isoform of Neuroglian (Islam et al., 2003). Neuroglian-GFP is a GFP exon trap in *Neuroglian* (Morin et al., 2001). Marked balancer chromosomes used for mutant analysis were *CyO, P{w+, actinGFP}* with the exception of dlg^{m52}, *y*– mutants, which were scored for yellow mouth hooks.

Generation of transgenic lines

The UAS-Gliotactin lines were generated using the full-length AE27.41 cDNA subcloned into the *Eco*RI site of the pP{UAST} transformation vector (Brand and Perrimon, 1993). To create the UAS-GliotactinHA lines, complementary oligonucleotides encoding two repeats of the HA epitope tag (amino acid sequence: YPYDVPDYA) and tailed with PflM1 restriction sites were subcloned into a unique *Pfl*MI site just before the PDZ-binding motif in the Gliotactin cDNA (AE2 7.41). The resulting AE27.41-HA construct was subcloned into pP{UAST}, pP{UAST-AE27.41-HA}. To generate UAS-GliotactinΔPDZ, PCR was used to amplify from an internal *Kpn*I site in the AE27.41-HA cDNA to a primer designed to delete the S/TXV PDZ-binding motif at the C-terminal tail and replace it with a stop codon followed by a *Kpn*I site. The original AE27.41 cDNA was digested with *Kpn*I to release the wild-type region and replaced with the PCR product. The resulting AE27.41-HA-ΔPDZ construct was subcloned into pP{UAST}, pP{UAST-AE27.41-HA-ΔPDZ}. Engineered constructs were injected into w^{1118} embryos using standard techniques, independent insertion lines were isolated and balanced.

Immunohistochemistry

Embryos and larval tissues were fixed and stained as described previously (Schulte et al., 2003) with the exception that third instar larvae were first dissected in 1× PBS and then fixed for 30 minutes before processing for immunofluorescence. Labeled samples were cleared through 90% glycerol and mounted in Vectashield (Vector Laboratories). For Fig. 5, images were collected on a Bio-Rad Radiance Plus confocal microscope (40× oil and 63× oil objective lenses). Single, 2 μm optical slices were recorded. Confocal files were processed with ImageJ 1.24 and Adobe Photoshop 5.5. For all other figures, a Deltavision Restoration microscope (Applied Precision) was used. Data was collected using a 60× (1.4 NA) oil-immersion lens using a CoolSnap HQ digital camera. Data from all wavelengths was collected for each 0.2 μm optical section before the next section was collected. SoftWorx (Applied Precision) software was used for deconvolution of 10-15 iterations using a point spread function calculated with 0.2 μm beads conjugated with Alexa Fluor 568 (Molecular Probes) mounted in Vectashield. Images were then exported to Photoshop 7 for generation of figures. False colouring using the fire LUT (look-up table) was done on individual channels saved in grayscale and imported into ImageJ.

Antibodies used in this study were: rabbit anti-Neurexin IV at 1:200 (Baumgartner et al., 1996), mouse anti-Dlg 4F3 at 1:300 (Parnas et al., 2001), rat anti-DE-cadherin at 1:50 (Oda et al., 1994), mouse anti-Coracle (9C and C615-16B cocktail) at 1:100 (Fehon et al., 1994), mouse anti-Neuroglian 1B7 at 1:300 (Bieber et al., 1989), mouse anti-Armadillo 7A1 at 1:5 (Riggleman et al., 1990), and mouse

anti-Gliotactin 1F6.3 at 1:100 (Auld et al., 1995) or rabbit anti-Gliotactin at 1:300 (Venema et al., 2004). All the following secondary antibodies were used at 1:300 dilution: goat anti-mouse Alexa Fluor 488 and Alexa Fluor 568, goat anti-rabbit Alexa Fluor 488 and Alexa Fluor 568, goat anti-rat Alexa Fluor 488 (Molecular Probes) and goat anti-mouse Cy-5, goat anti-rabbit Cy-5 (Abcam). Neuroglian staining was assessed with antibody staining in somatic Gliotactin clones and in wild-type animals using the Neuroglian-GFP exon-trap line (Genova and Fehon, 2003).

Ectopic expression and rescue experiment

Rescue experiments were carried out at 23°C and overexpression experiments carried out at 29°C. For overexpression studies in a wild-type background, daughterless-Gal4, apterous-GAL4 or patched-GAL4 were used to drive UAS-GliotactinHA or UAS-GliotactinΔPDZHA. For rescue and localization studies, the transgenic UAS strains were placed into a *Gli$^{\Delta 45}$/CyO{actinGFP}* background and then crossed with *w;Gli$^{\Delta 45}$/CyO{actinGFP}; daughterless-GAL4*. Approximately 2000 embryos were screened for each rescue experiment. For rescue experiments, the progeny of this cross were screened with a GFP dissecting microscope to identify first instar larval escapers. First instar larval escapers were allowed to mature to adulthood and scored.

The *Gli^{dv3}, FRT40A* chromosome and the generation of Gliotactin null clones in the imaginal wing disc was described previously (Venema et al., 2004). After fixation and immunofluorescence labeling, all non-mutant cells are marked with nuclear-localized GFP and regions lacking GFP were outlined and superimposed on the other channels to show the location of each clone.

Biochemical analysis

Membrane preparations were carried out essentially as described (Sullivan et al., 2000). Immunoprecipitations were carried out using Protein G agarose beads (Invitrogen) prebound with mouse anti-Gliotactin mAb 1F6.3, mouse anti-HA (BabCO), or mouse IgG (Jackson ImmunoResearch). Samples were incubated in 200-250 μl lysis buffer (10 mM Tris-HCl, 4 mM EDTA, 1 mM EGTA, 150 mM NaCl, 0.5% Triton X-100 OR 0.2% NP-40, 1 mM PMSF, 2 μg/ml leupeptin, 2 μg/ml pepstatin) using a range of free Ca^{2+} (0.0, 0.05, 0.1 and 0.2 μM free Ca^{2+}). Membrane preparations were isolated from: *w^{1118}* adults or OregonR embryos (150 μg) or *UAS-GliHA, daughterless-GAL4* embryos (20 μg). Free Ca^{2+} concentrations were set as described by (Davletov and Sudhof, 1993). Precipitated complexes were washed four or five times in 200 μl lysis buffer with the appropriate Ca^{2+} concentration and then subjected to western blot analysis using the following primary antibodies: mouse anti-HA (1:1000), rabbit anti-Neurexin IV (1:2000), mouse anti-Dlg 4F3 (1:500), rabbit anti-Dlg (1:2000), guinea-pig anti-Coracle (1/2000) or mouse anti-Gliotactin 1F3 (1:500). Secondary antibodies used included HRP-conjugated goat anti-mouse (1:10,000), HRP-conjugated goat anti-rabbit (1:5000) and HRP-conjugated goat anti-guinea pig (1:10,000).

GST pull-down assays

GST pull-down assays were carried out on membrane preparations essentially as with the immunoprecipitation assays above. GST fusions were created with the C-terminal domain of Gliotactin from the AE27.41 cDNA plus or minus the PDZ-binding motif using PCR amplification from the first amino acid after the transmembrane domain to either the stop codon or for GliΔPDZ ending the fourth amino acid from the end. The Shaker-GST fusion was generated by PCR of the C-terminal domain of the Shaker K^+ channel from pCasper MHC-CD8-GFP-Shaker (Zito et al., 1999). Each was fused in frame into pGEX-4T (*Eco*RI for Gliotactin and *Bam*HI for Shaker). GST protein was induced, purified on glutathione beads and quantified. 50-75 μg of each fusion protein or GST alone was bound to glutathione beads and used in pull-down assays with 150 μg of membrane preparations with solutions containing varying Ca^{2+} concentrations as outlined above.

In vitro pull-down assays were carried out as described (Kyba and Brock, 1998) with the TNT Coupled Reticulocyte Lysate Kit (Promega) with the Dlg-A cDNA to Dlg-A (Woods and Bryant, 1991). Each in vitro reaction was precleared with GST bound to glutathione beads. 5-10 μg GST alone or GST fusion protein was blocked with 2% BSA and then bound to 50% of the in vitro translation product. After extensive washing, proteins were separated by SDS-PAGE, and bands analyzed by western blot using a mAb to Dlg as described above.

We thank M, Bhat, P. Bryant, the Developmental Studies Hybridoma Bank, R. Fehon, M. Horscht, H. Oda, and E. Wieschaus for generously providing antibodies, stocks, and clones; the Bloomington Stock Center for fly stocks; J. Otte for technical support and M. Gilbert, C. Roskelley for helpful discussions and comments on the manuscript. This study was supported by a grant to V.J.A. from the Canadian Institute of Health Research. J.S. and C.M. were both supported by a studentship from the Rick Hansen Neurotrauma Initiative.

References

Auld, V. J., Fetter, R. D., Broadie, K. and Goodman, C. S. (1995). Gliotactin, a novel transmembrane protein on peripheral glia, is required to form the blood-nerve barrier in Drosophila. *Cell* **81**, 757-767.

Baumgartner, S., Littleton, J. T., Broadie, K., Bhat, M. A., Harbecke, R., Lengyel, J. A., Chiquet-Ehrismann, R., Prokop, A. and Bellen, H. J. (1996). A Drosophila neurexin is required for septate junction and blood-nerve barrier formation and function. *Cell* **87**, 1059-1068.

Bieber, A. J., Snow, P. M., Hortsch, M., Patel, N. H., Jacobs, J. R., Traquina, Z. R., Schilling, J. and Goodman, C. S. (1989). Drosophila neuroglian: a member of the immunoglobulin superfamily with extensive homology to the vertebrate neural adhesion molecule L1. *Cell* **59**, 447-460.

Boucard, A. A., Chubykin, A. A., Comoletti, D., Taylor, P. and Sudhof, T. C. (2005). A splice code for trans-synaptic cell adhesion mediated by binding of neuroligin 1 to alpha- and beta-neurexins. *Neuron* **48**, 229-236.

Brand, A. H. and Perrimon, N. (1993). Targeted gene expression as a means of altering cell fates and generating dominant phenotypes. *Development* **118**, 401-415.

Cronmiller, C. and Cummings, C. A. (1993). The daughterless gene product in Drosophila is a nuclear protein that is broadly expressed throughout the organism during development. *Mech. Dev.* **42**, 159-169.

Davletov, B. A. and Sudhof, T. C. (1993). A single C2 domain from synaptotagmin I is sufficient for high affinity Ca^{2+}/phospholipid binding. *J. Biol. Chem.* **268**, 26386-26390.

Dean, C., Scholl, F. G., Choih, J., DeMaria, S., Berger, J., Isacoff, E. and Scheiffele, P. (2003). Neurexin mediates the assembly of presynaptic terminals. *Nat. Neurosci.* **6**, 708-716.

Dresbach, T., Neeb, A., Meyer, G., Gundelfinger, E. D. and Brose, N. (2004). Synaptic targeting of neuroligin is independent of neurexin and SAP90/PSD95 binding. *Mol. Cell. Neurosci.* **27**, 227-235.

Faivre-Sarrailh, C., Banerjee, S., Li, J., Hortsch, M., Laval, M. and Bhat, M. A. (2004). Drosophila contactin, a homolog of vertebrate contactin, is required for septate junction organization and paracellular barrier function. *Development* **131**, 4931-4942.

Fehon, R. G., Dawson, I. A. and Artavanis-Tsakonas, S. (1994). A Drosophila homologue of membrane-skeleton protein 4.1 is associated with septate junctions and is encoded by the coracle gene. *Development* **120**, 545-557.

Fristrom, D. K. (1982). Septate junctions in imaginal disks of Drosophila: a model for the redistribution of septa during cell rearrangement. *J. Cell Biol.* **94**, 77-87.

Genova, J. L. and Fehon, R. G. (2003). Neuroglian, Gliotactin, and the Na+/K+ ATPase are essential for septate junction function in Drosophila. *J. Cell Biol.* **161**, 979-989.

Gilbert, M. M. and Auld, V. J. (2005). Evolution of clams (cholinesterase-like adhesion molecules): structure and function during development. *Front. Biosci.* **10**, 2177-2192.

Gilbert, M., Smith, J., Roskams, A. J. and Auld, V. J. (2001). Neuroligin 3 is a vertebrate gliotactin expressed in the olfactory ensheathing glia, a growth-promoting class of macroglia. *Glia* **34**, 151-164.

Hortsch, M. and Margolis, B. (2003). Septate and paranodal junctions: kissing cousins. *Trends Cell Biol.* **13**, 557-561.

Hough, C. D., Woods, D. F., Park, S. and Bryant, P. J. (1997). Organizing a functional junctional complex requires specific domains of the Drosophila MAGUK Discs large. *Genes Dev.* **11**, 3242-3253.

Hung, A. Y. and Sheng, M. (2002). PDZ domains: structural modules for protein complex assembly. *J. Biol. Chem.* **277**, 5699-5702.

Ichtchenko, K., Hata, Y., Nguyen, T., Ullrich, B., Missler, M., Moomaw, C. and Sudhof, T. C. (1995). Neuroligin 1, a splice site-specific ligand for beta-neurexins. *Cell* **81**, 435-443.

Ichtchenko, K., Nguyen, T. and Sudhof, T. C. (1996). Structures, alternative splicing, and neurexin binding of multiple neuroligins. *J. Biol. Chem.* **271**, 2676-2682.

Iida, J., Hirabayashi, S., Sato, Y. and Hata, Y. (2004). Synaptic scaffolding molecule is involved in the synaptic clustering of neuroligin. *Mol. Cell. Neurosci.* **27**, 497-508.

Irie, M., Hata, Y., Takeuchi, M., Ichtchenko, K., Toyoda, A., Hirao, K., Takai, Y., Rosahl, T. W. and Sudhof, T. C. (1997). Binding of neuroligins to PSD-95. *Science* **277**, 1511-1515.

Islam, R., Wei, S. Y., Chiu, W. H., Hortsch, M. and Hsu, J. C. (2003). Neuroglian activates Echinoid to antagonize the Drosophila EGF receptor signaling pathway. *Development* **130**, 2051-2059.

Koh, Y. H., Popova, E., Thomas, U., Griffith, L. C. and Budnik, V. (1999). Regulation of DLG localization at synapses by CaMKII-dependent phosphorylation. *Cell* **98**, 353-363.

Kurschner, C., Mermelstein, P. G., Holden, W. T. and Surmeier, D. J. (1998). CIPP, a novel multivalent PDZ domain protein, selectively interacts with Kir4.0 family members, NMDA receptor subunits, neurexins, and neuroligins. *Mol. Cell. Neurosci.* **11**, 161-172.

Kyba, M. and Brock, H. W. (1998). The Drosophila polycomb group protein Psc contacts ph and Pc through specific conserved domains. *Mol. Cell. Biol.* **18**, 2712-2720.

Llimargas, M., Strigini, M., Katidou, M., Karagogeos, D. and Casanova, J. (2004). Lachesin is a component of a septate junction-based mechanism that controls tube size and epithelial integrity in the Drosophila tracheal system. *Development* **131**, 181-190.

Mendoza, C., Olguin, P., Lafferte, G., Thomas, U., Ebitsch, S., Gundelfinger, E. D., Kukuljan, M. and Sierralta, J. (2003). Novel isoforms of Dlg are fundamental for neuronal development in Drosophila. *J. Neurosci.* **23**, 2093-2101.

Morin, X., Daneman, R., Zavortink, M. and Chia, W. (2001). A protein trap strategy to detect GFP-tagged proteins expressed from their endogenous loci in Drosophila. *Proc. Natl. Acad. Sci. USA* **98**, 15050-15055.

Noirot-Timothee, C., Graf, F. and Noirot, C. (1982). The specialization of septate

junctions in regions of tricellular junctions. II. Pleated septate junctions. *J. Ultrastruct. Res.* **78**, 152-165.

Oda, H., Uemura, T., Harada, Y., Iwai, Y. and Takeichi, M. (1994). A Drosophila homolog of cadherin associated with armadillo and essential for embryonic cell-cell adhesion. *Dev. Biol.* **165**, 716-726.

Parnas, D., Haghighi, A. P., Fetter, R. D., Kim, S. W. and Goodman, C. S. (2001). Regulation of postsynaptic structure and protein localization by the Rho-type guanine nucleotide exchange factor dPix. *Neuron* **32**, 415-424.

Peles, E. and Salzer, J. L. (2000). Molecular domains of myelinated axons. *Curr. Opin. Neurobiol.* **10**, 558-565.

Prange, O., Wong, T. P., Gerrow, K., Wang, Y. T. and El-Husseini, A. (2004). A balance between excitatory and inhibitory synapses is controlled by PSD-95 and neuroligin. *Proc. Natl. Acad. Sci. USA* **101**, 13915-13920.

Riggleman, B., Schedl, P. and Wieschaus, E. (1990). Spatial expression of the Drosophila segment polarity gene armadillo is posttranscriptionally regulated by wingless. *Cell* **63**, 549-560.

Schulte, J., Tepass, U. and Auld, V. J. (2003). Gliotactin, a novel marker of tricellular junctions, is necessary for septate junction development in Drosophila. *J. Cell Biol.* **161**, 991-1000.

Sullivan, W., Ashburner, M. and Hawley, R. S. (2000). *Drosophila Protocols*. Cold Spring Harbor: Cold Spring Harbor Laboratory Press.

Tejedor, F. J., Bokhari, A., Rogero, O., Gorczyca, M., Zhang, J., Kim, E., Sheng, M. and Budnik, V. (1997). Essential role for dlg in synaptic clustering of Shaker K+ channels in vivo. *J. Neurosci.* **17**, 152-159.

Tepass, U. and Hartenstein, V. (1994). The development of cellular junctions in the Drosophila embryo. *Dev. Biol.* **161**, 563-596.

Thomas, U., Ebitsch, S., Gorczyca, M., Koh, Y. H., Hough, C. D., Woods, D., Gundelfinger, E. D. and Budnik, V. (2000). Synaptic targeting and localization of discs-large is a stepwise process controlled by different domains of the protein. *Curr. Biol.* **10**, 1108-1117.

Tsigelny, I., Shindyalov, I. N., Bourne, P. E., Sudhof, T. C. and Taylor, P. (2000). Common EF-hand motifs in cholinesterases and neuroligins suggest a role for Ca^{2+} binding in cell surface associations. *Protein Sci.* **9**, 180-185.

Venema, D. R., Zeev-Ben-Mordehai, T. and Auld, V. J. (2004). Transient apical polarization of Gliotactin and Coracle is required for parallel alignment of wing hairs in Drosophila. *Dev. Biol.* **275**, 301-314.

Walker, D. C., MacKenzie, A., Hulbert, W. C. and Hogg, J. C. (1985). A re-assessment of the tricellular region of epithelial cell tight junctions in trachea of guinea pig. *Acta Anat. Basel* **122**, 35-38.

Woods, D. F. and Bryant, P. J. (1991). The discs-large tumor suppressor gene of Drosophila encodes a guanylate kinase homolog localized at septate junctions. *Cell* **66**, 451-464.

Woods, D. F., Hough, C., Peel, D., Callaini, G. and Bryant, P. J. (1996). Dlg protein is required for junction structure, cell polarity, and proliferation control in Drosophila epithelia. *J. Cell Biol.* **134**, 1469-1482.

Zito, K., Parnas, D., Fetter, R. D., Isacoff, E. Y. and Goodman, C. S. (1999). Watching a synapse grow: noninvasive confocal imaging of synaptic growth in Drosophila. *Neuron* **22**, 719-729.

Journal of Cell Science